BJA

British Journal of Anaesthesia, 128 (6): 1006–1018 (2022)

doi: 10.1016/j.bja.2022.01.010
Advance Access Publication Date: 9 February 2022
Neuroscience and Neuroanaesthesia

NEUROSCIENCE AND NEUROANAESTHESIA

Distinct EEG signatures differentiate unconsciousness and disconnection during anaesthesia and sleep

Cameron P. Casey[1], Sean Tanabe[1], Zahra Farahbakhsh[1], Margaret Parker[1], Amber Bo[1], Marissa White[1], Tyler Ballweg[1], Andrew Mcintosh[1], William Filbey[1], Yuri Saalmann[2], Robert A. Pearce[1] and Robert D. Sanders[3,4,5,*]

[1]Department of Anesthesiology, University of Wisconsin, Madison, WI, USA, [2]Department of Psychology, University of Wisconsin, Madison, WI, USA, [3]Specialty of Anaesthetics, University of Sydney, Camperdown, Sydney, Australia, [4]Department of Anaesthetics, Royal Prince Alfred Hospital, Camperdown, Sydney, Australia and [5]Institute of Academic Surgery, Royal Prince Alfred Hospital, Camperdown, Sydney, Australia

*Corresponding author. E-mail: robert.sanders@sydney.edu.au

This article is accompanied by an editorial: Consciousness and the outside world: is there anyone listening? by Hight & Sleigh, *Br J Anaesth* 2022:128:895–897, doi: 10.1016/j.bja.2022.02.001

Abstract

Background: How conscious experience becomes disconnected from the environment, or disappears, across arousal states is unknown. We sought to identify the neural correlates of sensory disconnection and unconsciousness using a novel serial awakening paradigm.

Methods: Volunteers were recruited for sedation with dexmedetomidine i.v., propofol i.v., or natural sleep with high-density EEG monitoring and serial awakenings to establish whether subjects were in states of disconnected consciousness or unconsciousness in the preceding 20 s. The primary outcome was classification of conscious states by occipital delta power (0.5–4 Hz). Secondary analyses included derivation (dexmedetomidine) and validation (sleep/propofol) studies of EEG signatures of conscious states.

Results: Occipital delta power differentiated disconnected and unconscious states for dexmedetomidine (area under the curve [AUC] for receiver operating characteristic 0.605 [95% confidence interval {CI}: 0.516; 0.694]) but not for sleep/propofol (AUC 0.512 [95% CI: 0.380; 0.645]). Distinct source localised signatures of sensory disconnection (AUC 0.999 [95% CI: 0.9954; 1.0000]) and unconsciousness (AUC 0.972 [95% CI: 0.9507; 0.9879]) were identified using support vector machine classification of dexmedetomidine data. These findings generalised to sleep/propofol (validation data set: sensory disconnection [AUC 0.743 {95% CI: 0.6784; 0.8050}]) and unconsciousness (AUC 0.622 [95% CI: 0.5176; 0.7238]). We identified that sensory disconnection was associated with broad spatial and spectral changes. In contrast, unconsciousness was associated with focal decreases in activity in anterior and posterior cingulate cortices.

Conclusions: These findings may enable novel monitors of the anaesthetic state that can distinguish sensory disconnection and unconsciousness, and these may provide novel insights into the biology of arousal.

Clinical trial registration: NCT03284307.

Keywords: consciousness; dexmedetomidine; EEG; machine learning; propofol; sensory disconnection; sleep

Received: 7 October 2021; **Accepted:** 5 January 2022

Editor's key points

- EEG correlates of sensory disconnection and consciousness could provide more sensitive monitors for anaesthesia and disorders of consciousness.
- A novel wake-up paradigm was used to identify EEG markers for various states of consciousness during infusion of dexmedetomidine or propofol and natural sleep in volunteers.
- Sensory disconnection and unconsciousness had distinct EEG signatures that were conserved across drug-induced and endogenous sleep states, with loss of consciousness associated with a reduction in activity within the anterior and posterior cingulate cortices.
- These findings contribute to our understanding of connectedness and consciousness and objective EEG measures of these phenomena that should improve monitors for clinical and research purposes.

Understanding the neural correlates of sensory awareness and conscious experience remains an open problem of great clinical and scientific importance. Without this knowledge, we are unable to monitor the anaesthetic state adequately or diagnose disorders of consciousness, particularly when responsiveness to the environment is impaired.[1–3] Perhaps most intriguing are the mechanisms by which consciousness becomes disconnected from the physical world in dreaming; practically, an understanding of the mechanisms of sensory disconnection would inform titration of anaesthetic dosing, development of therapies for insomnia, and improved neurological diagnosis.[4]

Prior research has used functional imaging technologies to study subjects who are sleeping or anaesthetised, contrasting baseline recordings with periods of putative 'unconsciousness' to identify neural correlates of consciousness.[5–9] Such studies have yielded a variety of markers that have been ascribed to consciousness; however, their methodologies have confounded consciousness with responsiveness making these results ambiguous. Unresponsive subjects may still be consciously aware of their environment or unaware of the environment, but they are still having a conscious experience, such as dreaming.[2,4,10] Furthermore, studies of anaesthesia that identify 'unconsciousness' based solely on the dose of anaesthetic given suffer from the additional confound of drug concentration.

These limitations have made it difficult to know which reported signatures are relevant to consciousness *per se* (i.e. the presence of phenomenological content) or perception of the external world. Serial awakening paradigms offer a way to approach this problem. A prior study made use of this paradigm to distinguish between dreaming consciousness and unconsciousness during sleep,[11] implicating a 'posterior hot zone'[12] of activity in the maintenance of consciousness. Whilst this made large improvements over previous experimental designs, the results were still limited in terms of external validity, as the data were only derived under natural sleep conditions and the authors did not comment on the mechanisms of sensory disconnection. Attempts to define similar changes with sedatives have had insufficient data to contrast dreaming consciousness and unconsciousness.[13]

In this study, we combined the serial awakening paradigm with titration of sedatives compared with natural sleep to probe for conserved, cross-state mechanisms of sensory disconnection and unconsciousness.[4] Additionally, we tested whether the neural correlates of consciousness included a posterior hot zone solely, as reported previously. By collecting reports of sensory disconnection and unconsciousness across multiple conditions and drug concentrations, we present generalisable signatures of connectedness and consciousness.

Our primary outcome was chosen as a simple measure of brain activity over the 'posterior hot zone', occipital delta power. *A priori*, we also planned exploratory analyses to identify if superior markers of the conscious state could be derived. Following prior reports of a 'posterior hot zone',[11,12] we conducted these secondary analyses in source space to obtain information on the regions involved in different conscious states. We hypothesised previously that perturbed noradrenergic signalling is a critical mechanism of sensory disconnection; hence, we focused our studies on dexmedetomidine (Dex). We also collected data on natural sleep and propofol (Prop), which we combined into a validation data set with which we could test the generalisability of our findings.

Methods

Subjects and drug administration

Subjects were enrolled in the Understanding Consciousness Connectedness and Intraoperative Unresponsiveness Study (NCT03284307). Participants were healthy volunteers between 18 and 40 yr old without prior contraindications to anaesthetics. The study was stopped prematurely because of study suspension by the COVID-19 pandemic and a change in institution of the primary investigator (RDS), at which time the primary Dex data set was complete. Data on ketamine were not included, as conscious reports could not be obtained by serial awakening from unresponsive subjects. The sevoflurane arm was removed before suspending recruitment because of concerns over whether verbal reports would be intelligible through a face mask (no subjects were recruited to this arm).

Anaesthesia was administered under the supervision of an anaesthetist to achieve a series of stable drug-dose plateaus. For Dex, a rapid infusion of 3.0 μg kg^{-1} h^{-1} was initially administered over a 10 min period followed by a 0.5 μg kg^{-1} h^{-1} maintenance infusion to achieve the first drug step. The second step was similarly achieved by a 10 min infusion of 3.0 μg kg^{-1} h^{-1} followed by a 1.5 μg kg^{-1} h^{-1} maintenance infusion. Plasma Dex concentration was estimated using pharmacokinetic/pharmacodynamic modelling.[14,15] Propofol administration involved target-controlled infusion using RUGLOOP (Ghent University, Ghent, Belgium) according to the model of Schnider and colleagues.[16] The duration of drug exposure was limited to 4 h for each experiment.

Serial wake reports

Subjects were allowed to rest with their eyes closed for 2–10 min at a time during drug sessions and 20–40 min at a time during sleep sessions without researcher intervention. Each rest period was concluded by a researcher calling the participant's name and initiating a brief structured interview consisting of questions designed to assess if the participant had been having a conscious experience directly before the name call and if the experience was connected to the environment

through the senses (Fig 1). Participant answers were evaluated by two members of the research team to code each wake report as connected consciousness (CC; conscious awareness of the environment), disconnected consciousness (DC; a conscious experience but no awareness of the environment, such as a dream), or unconsciousness (Unc; complete lack of experience). Both team members had to agree that a report could be unambiguously coded using the criteria in Figure 1 for it to be included in analysis. Selected examples of subject reports are available in Supplementary Figure S4. If the subjects were not rousable, they were not presumed unconscious and the attempted wake-up was excluded from the analysis. Likewise, internally conflicting reports for which an unambiguous state could not be assigned were also excluded from the analysis.

EEG data acquisition

High-density EEG data were collected using a NA300 EGI system with 256-channel gel caps. Electrodes were manually prepared with application of electrolyte gel to achieve

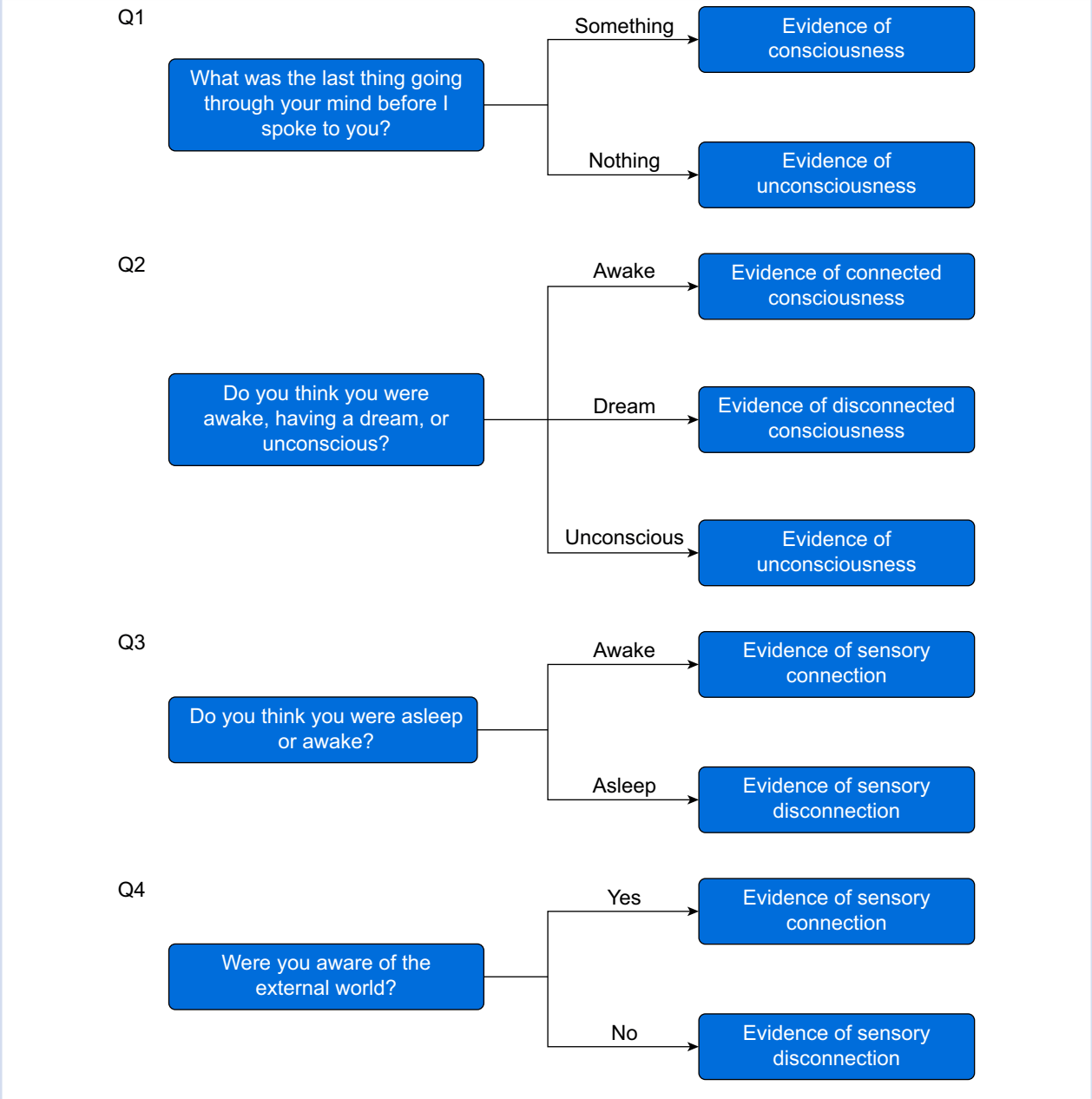

Fig 1. Wake report questions. Questions asked during wake reports to assess states of sensory connection and consciousness. Responses were evaluated by two members of the research team who had to agree on a state assignment of awake (W), connected consciousness (CC; conscious awareness of the environment), disconnected consciousness (DC; a conscious experience but no awareness of the environment, such as a dream), or unconsciousness (Unc; complete lack of experience) for a report to be included in the analyses.

electrode impedances <50 kΩ. Data were recorded using EGI Net Station Acquisition 5.4 software (Eugene, OR, USA).

Data processing was performed by a member of the research team experienced in EEG analysis whilst blinded to the assigned conscious state using EEGLAB.[17] Data were filtered between 0.1 and 55 Hz. Filtered data were then visually inspected for noisy channels and noisy epochs, which were removed. Independent component analysis was then computed using the InfoMax[18] algorithm, and components dominated by eye movements or muscle artifacts were rejected. After these cleaning steps, data were average referenced, and the last 20 s of data before the wake report was segmented out for analysis. Sensor-space power spectra were generated by computing the Welch power spectral density of the spline-based Laplacian transformed data.[19]

Primary outcome

Power spectral density in the delta band (1–4 Hz) was averaged at electrode Oz and tested for differences between conscious states (DC *vs* CC and Unc *vs* DC) using linear mixed effects models (LMEMs) as implemented in the R lme4 library[20] (see Statistical methods section). The predictive utility of the primary outcome was tested using empirical receiver operating characteristic (ROC) curves, which were summarised by the area under the curve (AUC) with bootstrapped 95% confidence intervals (CIs).

Source reconstruction

EEG data were imported into FieldTrip[21] and source reconstructed by frequency band using the eLORETA[22] algorithm. Frequency bands were specified as slow-wave activity (SWA; 0.5–1 Hz), delta (1–4 Hz), theta (4–8 Hz), alpha (8–14 Hz), beta (18–25 Hz), and gamma (28–55 Hz). An average brain model, taken from the SPM8 release (FieldTrip file cortex_20484.surf.gii), was used for the source model. The volume conductance model was a three-shell boundary element method model with conductances of 0.33, 0.0041, and 0.33 for skin, skull, and brain, respectively (FieldTrip file standard_bem.mat).

Statistical analysis

Source reconstructed data were analysed voxel-wise using LMEMs, in which the log-transformed power at each voxel was regressed on wake state and predicted plasma drug concentration with by-subject random intercepts and by-subject random slopes for predicted plasma drug concentration to account for non-independence of repeated measures from the same subject. For all analyses involving the Sleep data set, the baseline W coded data were used as the equivalent of CC, as the sleep condition does not have a W/CC distinction equivalent to that of the Dex or Prop condition. Wake state was treated as a dummy-coded variable to perform pairwise state contrasts. Drug concentration was treated as a continuous covariate to adjust for the non-specific effects of anaesthesia that are not relevant to connectedness or consciousness. *P*-values were generated using Type III analysis of variance with Kenward–Roger degrees of freedom for the *F*-test. To correct for multiple comparisons, *P*-values corresponding to voxels within the same frequency band were adjusted using the Benjamini–Hochberg false discovery rate (FDR) procedure. To ascribe anatomical labels to the significant results, we masked the significant voxels against the automated anatomical labelling (AAL) atlas[23] from SPM8.

Machine learning

Machine learning was performed separately for classification of DC *vs* CC and Unc *vs* DC wake reports, using Dex as a training set and Prop/Sleep as a test set. For the DC *vs* CC contrast, the source activation at each voxel across all frequency bands was included from training. These data were log transformed to improve normality and subjected to principal component analysis to reduce dimensionality of the highly collinear data. The relative predictive value of each principal component for classification was calculated using the random forest recursive feature elimination algorithm implemented in the R caret library.[24] Principal components with mean decrease in accuracy values greater than 0 were retained as training features. The number of features retained in each machine learning model is outlined in Supplementary Table S2.

Ensemble machine learning was performed by bootstrap aggregating 500 linear support vector machines (SVMs). To address the unbalanced nature of the training classes, balanced bootstrap samples were used to train each model. The *n* for each class was chosen as 50, the *n* of the smaller class (CC), such that each model was trained with a bootstrapped sample of 50 CC and 50 DC data points. The model cost tuning parameter was allowed to vary across models and was chosen from the range (0.1, 0.25, 0.5, 1, 2, 4, 8, 16, 32) based on the model that produced the largest kappa statistic. When applying the ensemble learner to the test set, each SVM produced a probability score for the DC/CC classification; these were averaged across all 500 models, and the class with the larger probability was chosen as the predicted class for the ensemble. The machine learning process for the Unc *vs* DC classification problem was identical to that used for DC *vs* CC, except that only seed voxels for beta and delta bands from significant regions of interest (ROI) of the beta/delta ratio were included. For quantification of SVM ensemble performance, we calculated 95% CIs for the AUC of each ROC and compared against chance levels of 0.5.

Results

States of consciousness show similar EEG signatures across conditions

To disentangle the constructs of connectedness and consciousness, we recruited healthy volunteers to record high-density EEG (256 channels) with i.v. infusion of Dex (n=20) or Prop (n=6), or during natural sleep (n=15). Dexmedetomidine and Prop were titrated to multiple drug steps to promote increasing somnolence (Fig 2a). Totals of 398, 104, and 202 wake-ups were attempted for Dex, Prop, and Sleep conditions, respectively. Because of instances in which the subjects did not give a verbal report or the report was ambiguous, not all attempted wake-ups resulted in usable data. The numbers of wake-ups analysed were 330 for Dex, 88 for Prop, and 188 for Sleep (see Fig 2b legend for additional details). Frequency of each reported state (W, CC, DC, or Unc) varied across experimental conditions (Fig 2b), predicted plasma drug concentration (Fig 2c), and responsiveness (Fig 2d); however, each state was observed, to some degree, across each of these variables.

Spectral analysis of the EEG data from the 20 s before each wake report showed similar (although not identical) patterns of activity in W/CC states and DC/Unc states (Fig 3a). The most notable qualitative differences between connected (W/CC) and disconnected (DC) or unconscious (Unc) states were

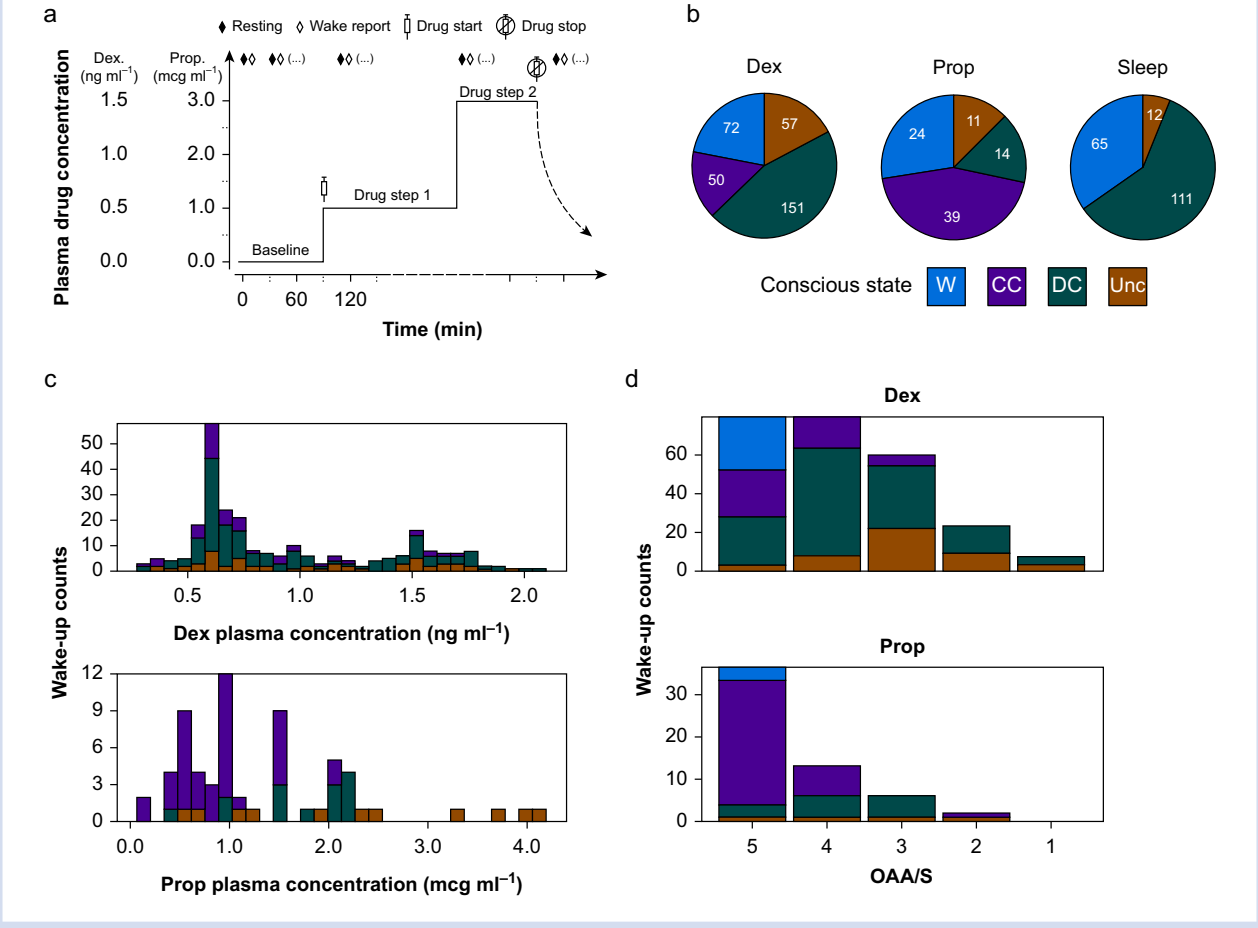

Fig 2. Drug administration and wake report collection. a: Hypothetical drug dosing diagram illustrating experimental paradigm for serial wake reports, which results in multiple wake reports per subject. b: Distribution of analysed wake reports by state in each experimental condition. States coded as W (wake; connected consciousness pre-drug), CC (connected consciousness with drug), DC (disconnected consciousness), or Unc (unconsciousness). Additional wake-ups were attempted (Att), but the data were unusable because of either no verbal response (NVR) or ambiguous answers that could not be confidently classified (Amb). The final analysed counts by condition were (Dex) $330{=}398_{Att}{-}12_{NVR}{-}56_{Amb}$, (Prop) $88{=}104_{Att}{-}7_{NVR}{-}9_{Amb}$, and (Sleep) $188{=}202_{Att}{-}2_{NVR}{-}12_{Amb}$. c: Distribution of wake states across modelled plasma drug concentrations of Dex and Prop. d: Distribution of wake states by level of responsiveness as assessed by the OAAS. Dex, dexmedetomidine; OAAS, Observer's Assessment of Alertness/Sedation; Prop, propofol.

reduced high-frequency power (16–55 Hz) and posterior alpha power (9–12 Hz) and increased low-frequency power (0.5–9 Hz) with DC/Unc states.

Primary outcome

Occipital delta power showed a linear relationship with conscious state (Fig 3b). Using a linear mixed effects model with by-subject random effects (intercept and predicted plasma drug concentration) and fixed effects for conscious state and predicted plasma drug concentration, we compared the effect of conscious state on delta power using DC as the reference condition. Mean delta power during CC was 65.2% of that recorded during DC ($P<0.001$), whilst mean Unc delta power was 124.2% of that recorded during DC ($P=0.030$) (Fig 3c and Supplementary Table S1). Occipital delta power showed a weak classification for disconnected and unconscious states (Fig 3d), the primary outcome, for Dex (AUC for the ROC 0.605 [95% CI: 0.516; 0.694]). However, this effect was not evident for Sleep/Prop (AUC 0.512 [95% CI: 0.380; 0.645]); hence, this marker is unlikely to represent a reliable marker of conscious state for clinical application. To further interrogate the signatures of connectedness and consciousness, we source reconstructed the EEG data, allowing us to investigate the anatomical sources of spectral changes.

Disconnected consciousness differs from connected consciousness

Our primary motivation was to investigate generalisable EEG signatures of connectedness and consciousness. We adopted a machine learning analytical approach, in which we divided the data into a discovery set for Dex and a generalisability test set for Prop and Sleep. We chose the α_2 adrenoceptor agonist Dex for the discovery data set to identify whether perturbed noradrenergic signalling offers a conserved mechanism of sensory disconnection based on reduced locus coeruleus activity in the disconnected state of sleep[25] and on

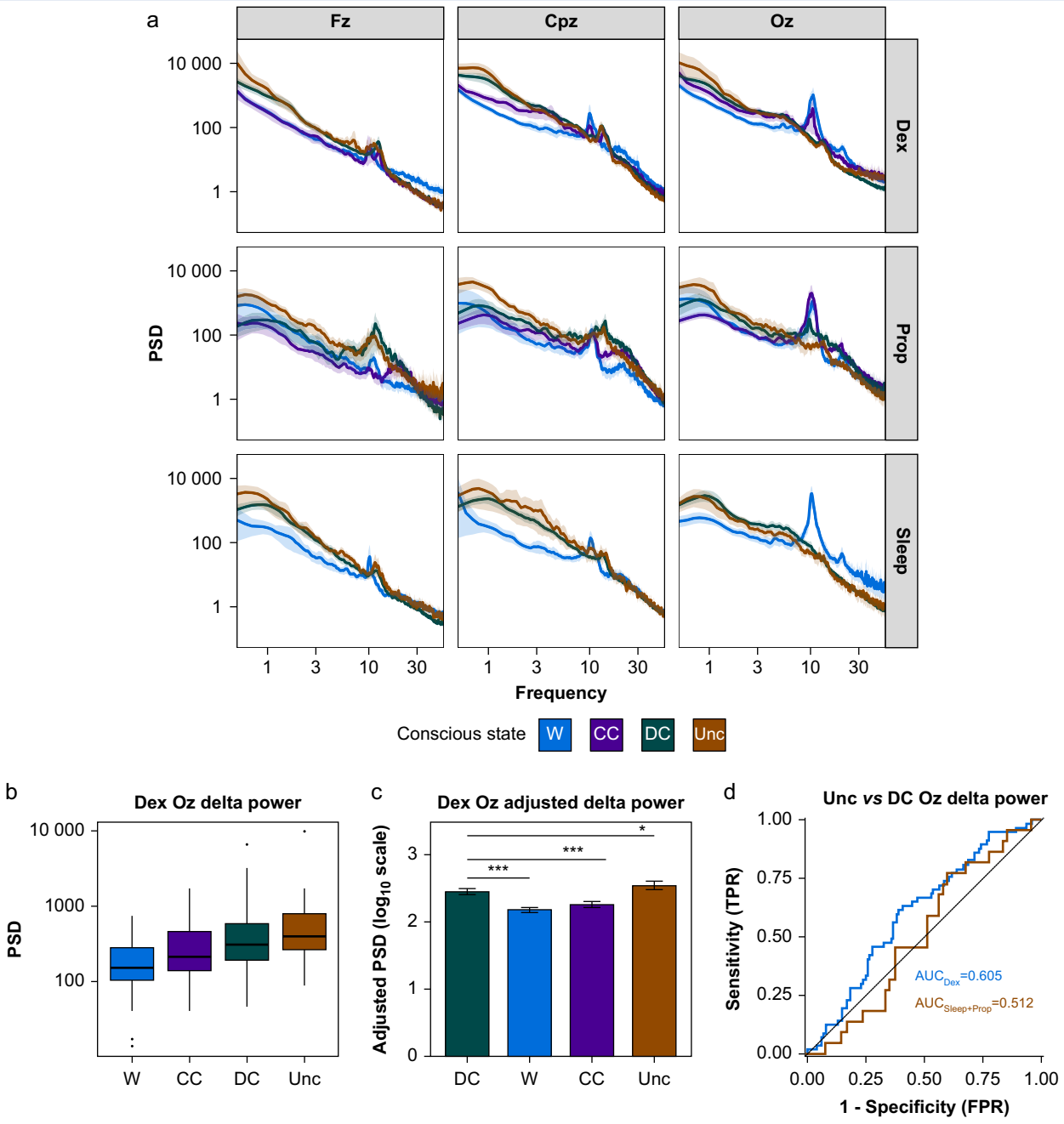

Fig 3. Scalp-level EEG power analysis. a: Scalp-level power spectral density (PSD) by frequency (average reference and Laplacian transformed) at the canonical electrodes Fz (frontal midline), Cpz (central midline), and Oz (occipital midline) across conditions. Experimental conditions show similar patterns of activity with a notable loss of occipital alpha (~10 Hz) in DC and Unc relative to W and CC, and an increase in low-frequency activity (0.5–9 Hz) and decrease in high-frequency activity (16–55 Hz) across electrodes. b: Box plots comparing mean delta PSD at Oz across wake-ups for Dex. c: Bar plot of the adjusted delta PSD values (on a $\log_{10}$ scale) from a LMEM contrasting DC against all other states whilst controlling for predicted plasma drug concentration and subject-specific effects. Error bars represent bootstrapped standard errors. *P<0.05, ***P<0.001. d: Empirical ROC curves for classifying Unc *vs* DC for Dex (red) and Sleep/Prop (purple). Black line represents chance performance (AUC=0.5). AUC, area under the curve; CC, connected consciousness; DC, disconnected consciousness; Dex, dexmedetomidine; FPR, false positive rate; LMEM, linear mixed effects model; Prop, propofol; ROC, receiver operating characteristic; TPR, true positive rate; Unc, unconsciousness.

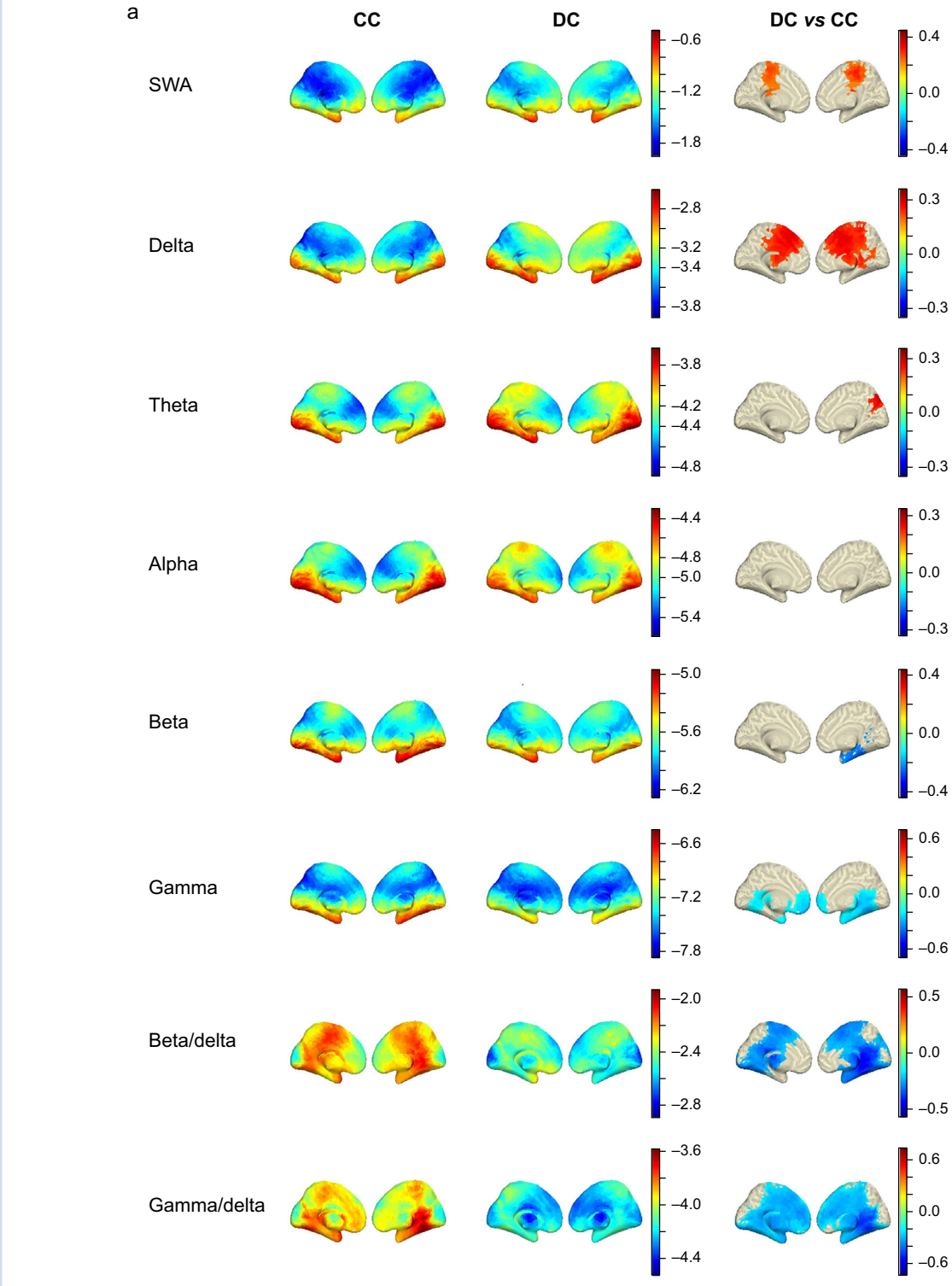

Fig 4. Disconnected consciousness compared with connected consciousness across frequency bands. a: Medial view of voxel-wise predicted power (log_{10} scale colour coded) from LMEMs for CC (left column) and DC (middle column) across frequency bands. Right column shows differences between DC and CC states for all significant voxels after FDR correction for multiple comparisons. b: Same as in (a) but showing lateral view. c: Depiction of machine learning approach used to classify DC and CC data. Briefly, Dex data were used as a training set and subjected to PCA for dimensionality reduction before feature selection. The Prop and Sleep test data were projected into the same feature space. Training features were used to generate an ensemble of 500 SVMs, each trained using a different subset of the training data, bootstrap sampled with balanced class representation. The ensemble was applied to the test data by averaging the probability scores of all

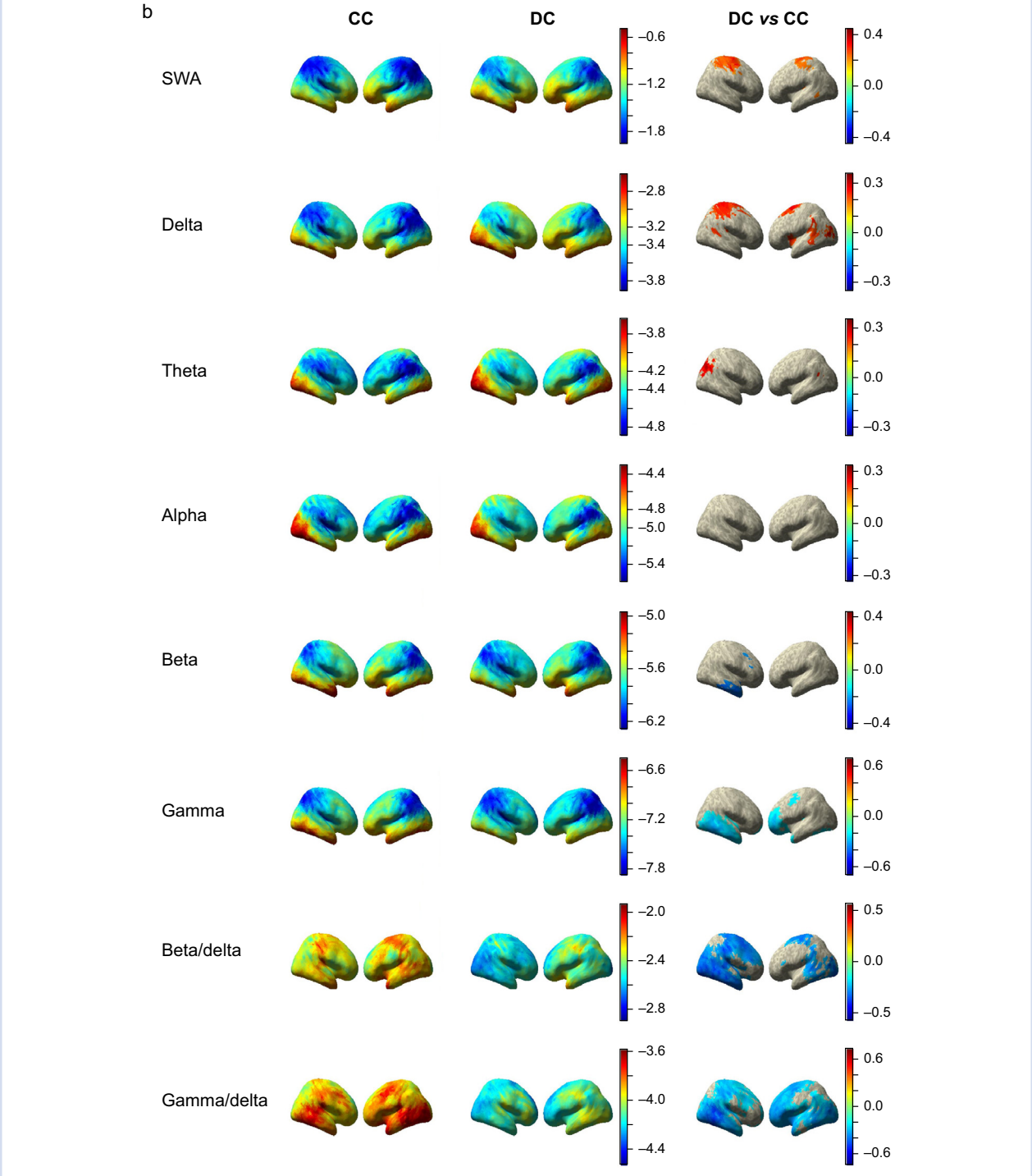

Fig 4. Continued

500 models and selecting the class with the higher average probability. d: ROC curves for the ensemble learner, training using all bands except alpha, applied to the training set and test set with AUC quantification. The black line represents chance performance (AUC=0.5). AUC, area under the curve; CC, connected consciousness; DC, disconnected consciousness; Dex, dexmedetomidine; FDR, false discovery rate; LMEM, linear mixed effects model; PCA, principal component analysis; Prop, propofol; ROC, receiver operating characteristic; SVM, support vector machine; SWA, slow-wave activity.

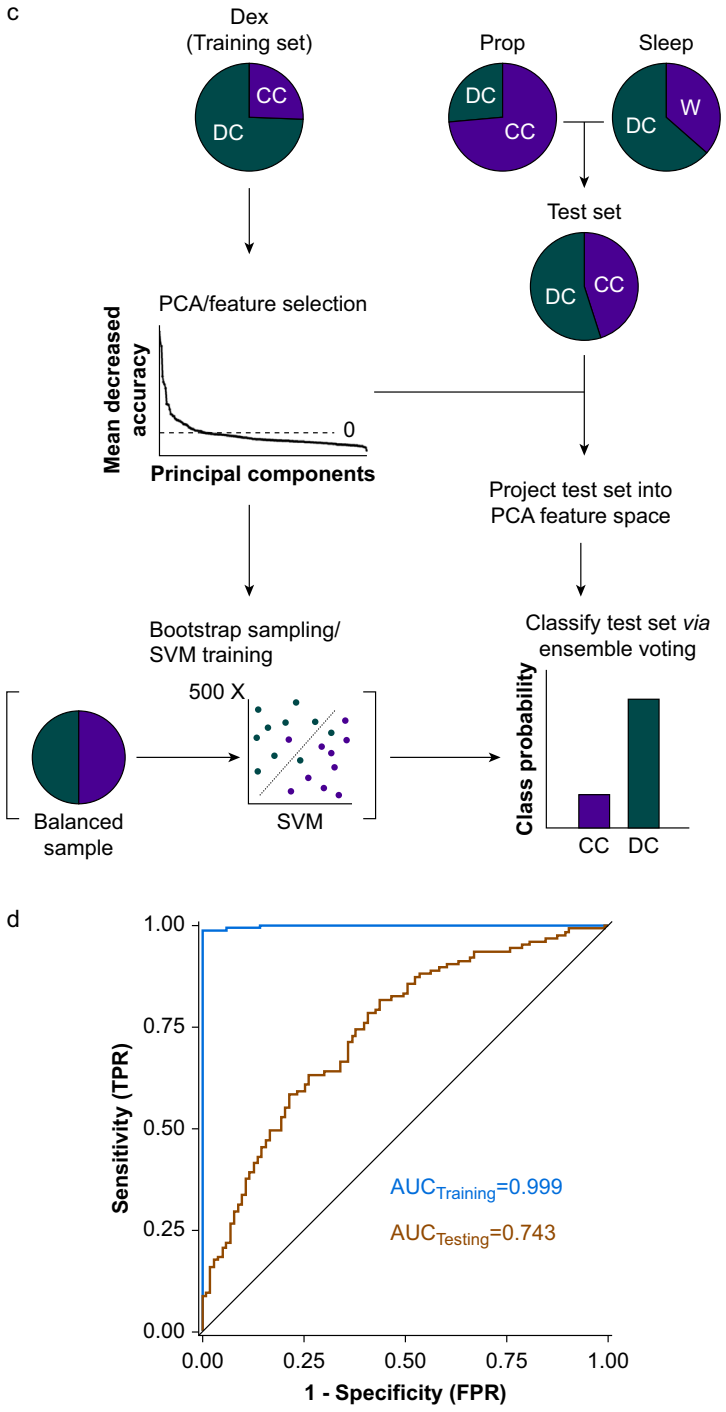

Fig 4. Continued

the characteristics of norepinephrine to provide gain across the sensory cortical hierarchy.[26] Within the Dex discovery set, we performed a source space voxel-wise analysis, making use of LMEMs to predict spectral power as a function of wake report state whilst adjusting for predicted plasma drug concentration, overcoming a major limitation of prior studies of that did not dissect non-specific drug effects from conscious state.

Our modelling approach highlighted significant differences in cortical rhythms in the SWA, delta, theta, beta, and gamma bands (Fig 4a and b), which was greater in fronto-medial cortex and surrounding the superior portion of the central sulcus in

the DC condition ($P<0.05$; FDR corrected). We also observed a small posterior cluster in the right hemisphere of increased theta activity in DC compared with CC, consistent with cuneus/precuneus. In contrast to the increase in lower frequencies, the higher beta and gamma frequencies were significantly decreased in DC relative to CC. Beta showed decreases in the right temporal lobe, whilst gamma decreased bilaterally in frontal and temporal lobes. Prior research defined a posterior hot zone of activity based on reductions in high-frequency power and increased low-frequency power in unconsciousness relative to dreaming in sleep.[11] We tested the specificity of this marker by operationalising it as a beta/delta ratio or a gamma/delta ratio. The ratio of high-frequency to low-frequency activity may represent how active an area of cortex is, given that cerebral metabolism positively correlates with high-frequency rhythms and negatively correlates with low-frequency frequencies.[27,28] Both ratios demonstrated more widespread changes in DC *vs* CC than any of their constituent frequency bands.

We further investigated the predictive utility and generalisability of these power bands by using them as predictors in a machine learning classifier of sensory disconnection. We trained an ensemble of 500 SVMs to classify the Dex DC and CC data using all frequency bands except alpha (which was omitted because of no significant effects in the DC *vs* CC contrast), and we tested its performance on the Prop and Sleep data (Fig 4c). The ensemble had near-perfect performance within the training set (AUC 0.999 [95% CI: 0.9954; 1.0000]) and performed well above chance levels in the test set (AUC 0.743 [95% CI: 0.6784; 0.8050]), demonstrating generalisability of the EEG signatures of disconnection observed for Dex (Fig 4d). Inclusion of the alpha band did not substantially influence the model (Supplementary Fig. S3a).

Unconsciousness differs from disconnected consciousness in beta/delta activity

In contrast to the broad spectral changes observed when contrasting DC and CC states, the differences between Unc and DC were much more specific. Unconsciousness showed significant reductions in beta/delta ratio in a bilateral set of medial anterior and posterior voxels and a lateral left hemispheric parietal cluster (Fig 5a). These regions correspond with anterior cingulate cortex (ACC), middle cingulate cortex and posterior cingulate cortex (PCC), and left supramarginal gyrus, respectively. To test the generalisability of these clusters as markers of unconsciousness, we defined ROI as the average activity of all voxels within 10 mm around the centroid of each cluster observed in the Dex data set (Supplementary Table S3). Modelling the beta/delta power at these ROI from the independent Prop and Sleep data showed similar results to the Dex data (Fig 5b and Supplementary Table S4). The one exception was the left parietal ROI, which was consistent for Dex and Prop but not for Sleep. Beta/delta power within the anterior and posterior medial clusters during Unc ranged from 16.7% to 53.2% of that recorded during DC (see Supplementary Table S4 for specific percentages in each cluster and condition). The non-significant results from the contrast of Unc and DC can be found in Supplementary Figure S2.

We also applied our ensemble SVM machine learning approach to these significant ROI using the same methodology as described for the DC *vs* CC classification (Fig 4c). An exception was that for this model, we only trained our model using beta/delta activity from voxels that were included as part of the ROI (the same voxels shown in Fig 5b). Again, the ensemble performed nearly perfectly within the training set (AUC 0.972 [95% CI: 0.9507; 0.9879]), but it also performed above chance levels in the independent Prop and Sleep test sets (AUC 0.622 [95% CI: 0.5176; 0.7238]) (Fig 5c). These results again support the generalisability and predictive utility of our findings in identifying unconsciousness under variable conditions. Because the left parietal ROI was not significant in the sleep condition, we performed a sensitivity analysis, in which the ensemble was trained using only the four medial ROI that were consistent across all conditions. This model performed comparably with the model with all five ROI (AUC 0.635 [95% CI: 0.5158; 0.7478]) (Supplementary Fig. S3b).

Discussion

Diffuse increases in delta and SWA and widespread suppression of gamma and beta bands are associated with anaesthetic drugs and non-rapid eye movement sleep.[5 29–32] Unfortunately, because of lack of subjective reports, these markers have often been assumed to be markers of unconsciousness. Our data suggest that these broad spectral changes are more accurately described as markers of sensory disconnection, whilst more focal changes within the cingulate cortex are markers for loss of consciousness. However, the simple marker of occipital delta power did not show adequate classification of the conscious state across anaesthetics and sleep.

The PCC is a core node of the default mode network (DMN), is highly active during autobiographical memory recall and introspection, and has been implicated in a posterior hot zone proposed to represent the neural correlates of consciousness.[12,33,34] The ACC is also part of the anterior DMN,[35,36] and it has been proposed to be a key node supporting consciousness in the global neuronal workspace model.[37,38] Both regions have been associated with deficits in consciousness individually.[33,39] Our data suggest that both anterior and posterior cingulate regions of the DMN are critical for consciousness, challenging the recent notion of a 'posterior hot zone'.[6] Moreover, recent fMRI studies have shown reductions in DMN activation during behavioural unresponsiveness for multiple anaesthetics and unresponsive wakefulness syndrome, and a recent positron emission tomography (PET) study identified reduced activity in ACC and PCC in unresponsive anaesthetised and sleeping subjects.[13,40] However, because of the limitations of responsiveness measurements, the authors were unable to conclude that these reductions were indicative of unconsciousness *per se*, as opposed to disconnected or covert consciousness. Our data build on this work by showing that reduced activity in these DMN nodes is associated with unconsciousness.

Our work is a significant advance on prior work as we work to disentangle disconnected conscious-dream states from unconsciousness.[13] Prior studies that claimed to study consciousness used unresponsiveness as a marker of unconsciousness. We have attempted to overcome this substantial limitation by using patient report to verify conscious state. These prior studies did not consider the confounding induced by changing drug concentrations. We adjusted for changes in drug concentrations in our models to remove non-specific drug effects from our analyses and focus our results on the change in conscious state.

Potential limitations in this study stem from our dependence on subjective reports to define the subjects' internal state. It is impossible to rule out subject error in reporting their

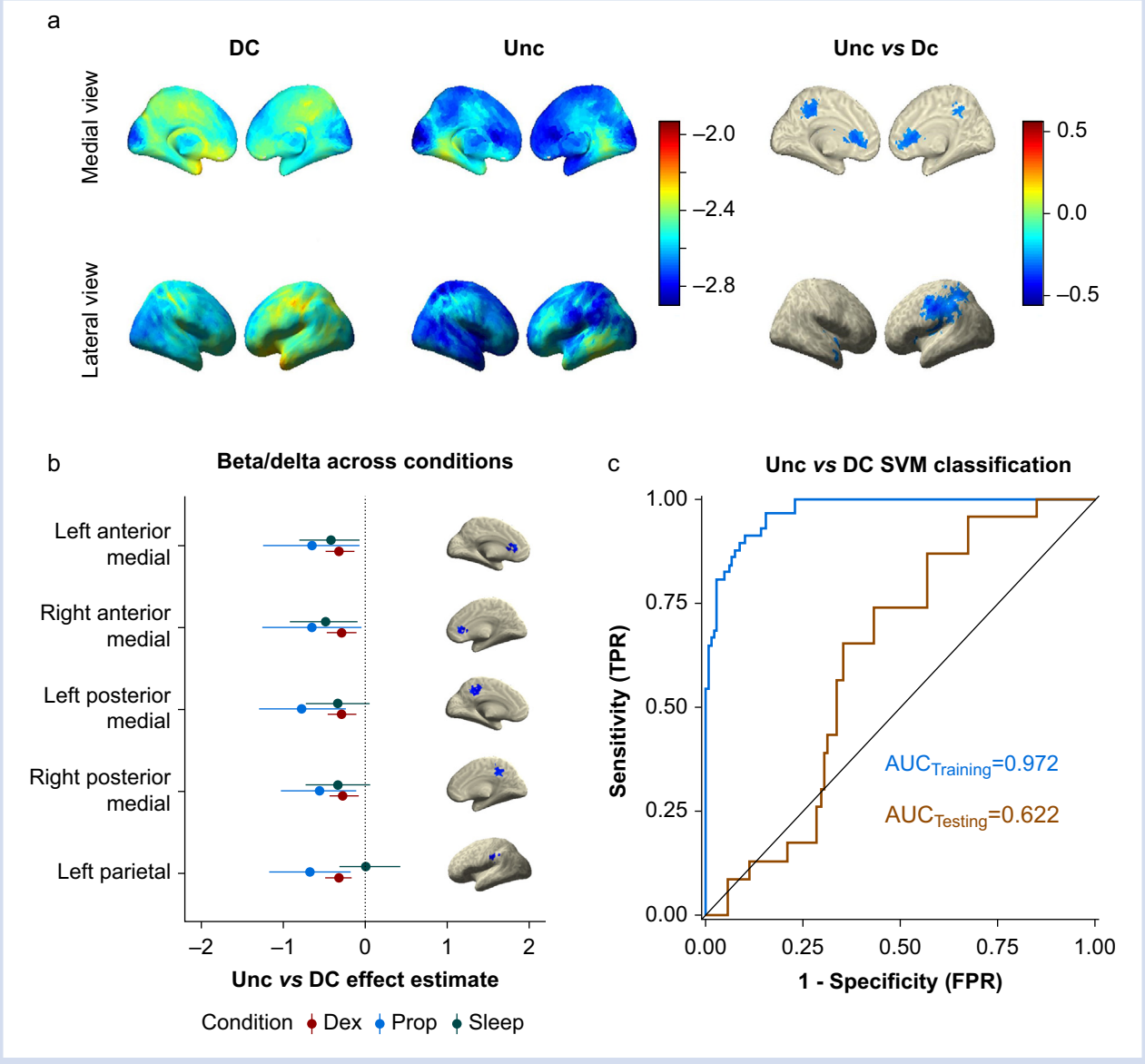

Fig 5. Unconsciousness compared with disconnected consciousness using beta/delta ratio. a: Voxel-wise predicted power (log_{10} scale colour coded) from LMEMs for DC (left column) and Unc (middle column) using beta/delta ratio. Right column shows differences between Unc and DC states for all significant voxels after FDR correction for multiple comparisons. b: Unc *vs* DC effect estimates of beta/delta activity with bootstrapped 95% confidence intervals comparing experimental conditions within select ROI. Anterior medial and posterior medial cortex ROI show similar effects across all three conditions. The left parietal cortex ROI was consistent between Dex and Prop, but it failed to generalise for Sleep data. c: ROC curves for the ensemble learner, training using beta/delta activity in the five ROI shown in (c), applied to the training set and test set with AUC quantification. The black line represents chance performance (AUC=0.5). AUC, area under the curve; DC, disconnected consciousness; Dex, dexmedetomidine; FDR, false discovery rate; LMEM, linear mixed effects model; Prop, propofol; ROC, receiver operating characteristic; ROI, regions of interest; SVM, support vector machine; Unc, unconsciousness.

state of consciousness. This is a substantial limitation to all attempts to study consciousness and a primary motivation for the current study. Experiments with pharmacological interventions also run the risk of increasing self-report error because of memory interference. We reason that miscoded data attributable to report error are only likely to increase the variance in our LMEMs, which could lead to more false-negative but not more false-positive results. Similarly, such miscoded data points would be expected to lower the estimated accuracy of our machine learning classifiers. We believe that, if such errors are present, results that achieve statistical significance in spite of them are certainly robust.

We also acknowledge the limited spatial specificity of EEG technology. In principle, this adds uncertainty to the anatomical sources of our findings. However, the overlap with prior findings using other modalities (e.g. PET and fMRI) gives us confidence in these results, although these prior studies could not distinguish disconnected conscious and unconscious states.

Our findings provide evidence that sensory disconnection and unconsciousness have distinct EEG signatures that are conserved across drug-induced and endogenous sleep states. Sensory disconnection was accompanied by widespread alterations in EEG activity across many frequency bands, whilst loss of consciousness was associated with a more specific reduction in activity within the ACC and PCC. This research is an important step in disentangling and quantifying the constructs of connectedness and consciousness, which are necessary for progressing our understanding of these fundamental phenomena and our ability to measure them objectively for clinical and research purposes.

Authors' contributions

Study conception: RDS
Experiment design: RDS
Data analytic approaches design: CPC, YS, RAP, RDS
Study management: RDS, RAP
Anaesthesia administration: WF, RDS
EEG and wake report data collection: CPC, ZF, ST, MP, AB, MW, TB, AM, RDS
Conducting of data analytic approaches: CPC
Writing of paper: CPC, RDS

Acknowledgements

The authors are grateful to the advice from Giulio Tononi, Brady Reidner, David Plante, and Melanie Boly (University of Wisconsin, Madison, WI, USA) when planning this project and for loan of the EEG equipment. The authors acknowledge Michel M. R. F. Struys and Tom De Smet from The University Medical Center Groningen (Groningen, The Netherlands) and Ghent University (Ghent, Belgium) for their assistance with RUGLOOP and infusion pump technology. Anthony Absalom (The University Medical Center Groningen) provided advice on pharmacokinetic modelling of dexmedetomidine concentrations.

Declarations of interest

RDS is a member of the board of the British Journal of Anaesthesia. The authors declare that they have no conflicts of interest.

Funding

Department of Anesthesiology, University of Wisconsin; US National Institutes of Health (1R01 NS117901).

Appendix A. Supplementary data

Supplementary data to this article can be found online at https://doi.org/10.1016/j.bja.2022.01.010.

References

1. Boly M, Sanders RD, Mashour GA, Laureys S. Consciousness and responsiveness: lessons from anaesthesia and the vegetative state. *Curr Opin Anaesthesiol* 2013; **26**: 444–9
2. Kotsovolis G, Komninos G. Awareness during anesthesia: how sure can we be that the patient is sleeping indeed? *Hippokratia* 2009; **13**: 83–9
3. Cascella M. Mechanisms underlying brain monitoring during anesthesia: limitations, possible improvements, and perspectives. *Korean J Anesthesiol* 2016; **69**: 113–20
4. Sanders RD, Tononi G, Laureys S, Sleigh JW. Unresponsiveness ≠ unconsciousness. *Anesthesiology* 2012; **116**: 946–59
5. Purdon PL, Pierce ET, Mukamel EA, et al. Electroencephalogram signatures of loss and recovery of consciousness from propofol. *Proc Natl Acad Sci U S A* 2013; **110**: E1142–51
6. Noreika V, Jylhänkangas L, Móró L, et al. Consciousness lost and found: subjective experiences in an unresponsive state. *Brain Cogn* 2011; **77**: 327–34
7. Ku S-W, Lee U, Noh G-J, Jun I-G, Mashour GA. Preferential inhibition of frontal-to-parietal feedback connectivity is a neurophysiologic correlate of general anesthesia in surgical patients. *PLoS One* 2011; **6**, e25155
8. Lee U, Ku S, Noh G, Baek S, Choi B, Mashour GA. Disruption of frontal-parietal communication by ketamine, propofol, and sevoflurane. *Anesthesiology* 2013; **118**: 1264–75
9. Långsjö JW, Alkire MT, Kaskinoro K, et al. Returning from oblivion: imaging the neural core of consciousness. *J Neurosci* 2012; **32**: 4935–43
10. Sanders RD, Gaskell A, Raz A, et al. Incidence of connected consciousness after tracheal intubation: a prospective, international, multicenter cohort study of the isolated forearm technique. *Anesthesiology* 2017; **126**: 214–22
11. Siclari F, Baird B, Perogamvros L, et al. The neural correlates of dreaming. *Nat Neurosci* 2017; **20**: 872–8
12. Boly M, Massimini M, Tsuchiya N, Postle BR, Koch C, Tononi G. Are the neural correlates of consciousness in the front or in the back of the cerebral cortex? Clinical and neuroimaging evidence. *J Neurosci* 2017; **37**: 9603–13
13. Scheinin A, Kantonen O, Alkire M, et al. Foundations of human consciousness: imaging the twilight zone. *J Neurosci* 2021; **41**: 1769–78
14. Bailey JM, Shafer SL. A simple analytical solution to the three-compartment pharmacokinetic model suitable for computer-controlled infusion pumps. *IEEE Trans Biomed Eng* 1991; **38**: 522–5
15. Hannivoort LN, Eleveld DJ, Proost JH, et al. Development of an optimized pharmacokinetic model of dexmedetomidine using target-controlled infusion in healthy volunteers. *Anesthesiology* 2015; **123**: 357–67
16. Schnider TW, Minto CF, Gambus PL, et al. The influence of method of administration and covariates on the pharmacokinetics of propofol in adult volunteers. *Anesthesiology* 1998; **88**: 1170–82
17. Delorme A, Makeig S. EEGLAB: an open source toolbox for analysis of single-trial EEG dynamics including independent component analysis. *J Neurosci Methods* 2004; **134**: 9–21
18. Bell AJ, Sejnowski TJ. An information-maximization approach to blind separation and blind deconvolution. *Neural Comput* 1995; **7**: 1129–59
19. Welch PD. The use of fast Fourier transform for the estimation of power spectra: a method based on time averaging over short, modified periodograms. *IEEE Trans Audio Electroacoust* 1967; **15**: 70–3
20. Bates D, et al. Fitting linear mixed-effects models using lme4. *J Stat Softw* 2015; **67**: 1–48. https://doi.org/10.18637/jss.v067.i01
21. Oostenveld R, Fries P, Maris E, Schoffelen J-M. FieldTrip: open source software for advanced analysis of MEG, EEG,

and invasive electrophysiological data. *Comput Intell Neurosci* 2011; **2011**: 156869
22. Pascual-Marqui RD, Lehmann D, Koukkou M, et al. Assessing interactions in the brain with exact low-resolution electromagnetic tomography. *Philos Trans R Soc A Math Phys Eng Sci* 2011; **369**: 3768–84
23. Rolls ET, Huang CC, Lin CP, Feng J, Joliot M. Automated anatomical labelling atlas 3. *Neuroimage* 2020; **206**: 116189
24. Kuhn M. Building predictive models in R using the caret package. *J Stat Softw* 2008; **28**: 1–26. https://doi.org/10.18637/jss.v028.i05
25. Aston-Jones G, Bloom FE. Activity of norepinephrine-containing locus coeruleus neurons in behaving rats anticipates fluctuations in the sleep-waking cycle. *J Neurosci* 1981; **1**: 876–86
26. Sanders RD, Casey C, Saalmann YB. Predictive coding as a model of sensory disconnection: relevance to anaesthetic mechanisms. *Br J Anaesth* 2021; **126**: 37–40
27. Nishida M, Juhász C, Sood S, Chugani HT, Asano E. Cortical glucose metabolism positively correlates with gamma-oscillations in nonlesional focal epilepsy. *Neuroimage* 2008; **42**: 1275–84
28. Wisor JP, Rempe MJ, Schmidt MA, Moore ME, Clegern WC. Sleep slow-wave activity regulates cerebral glycolytic metabolism. *Cereb Cortex* 2013; **23**: 1978–87
29. Brancaccio A, Tabarelli D, Bigica M, Baldauf D. Cortical source localization of sleep-stage specific oscillatory activity. *Sci Rep* 2020; **10**: 1–15
30. Akeju O, Pavone KJ, Westover MB, et al. A comparison of propofol- and dexmedetomidine-induced electroenceph alogram dynamics using spectral and coherence analysis. *Anesthesiology* 2014; **121**: 978–89
31. Marzano C, Moroni F, Gorgoni M, Nobili L, Ferrara M, De Gennaro L. How we fall asleep: regional and temporal differences in electroencephalographic synchronization at sleep onset. *Sleep Med* 2013; **14**: 1112–22
32. Purdon PL, Sampson A, Pavone KJ, Brown EN. Clinical electroencephalography for anesthesiologists. *Anesthesiology* 2015; **123**: 937–60
33. Vogt BA, Laureys S. Posterior cingulate, precuneal and retrosplenial cortices: cytology and components of the neural network correlates of consciousness. *Prog Brain Res* 2005; **150**: 205–17
34. Koch C, Massimini M, Boly M, Tononi G. Neural correlates of consciousness: progress and problems. *Nat Rev Neurosci* 2016; **17**: 307–21
35. Buckner RL, Andrews-Hanna JR, Schacter DL. The brain's default network: anatomy, function, and relevance to disease. *Ann N Y Acad Sci* 2008; **1124**: 1–38
36. Carter CS, Botvinick MM, Cohen JD. The contribution of the anterior cingulate cortex to executive processes in cognition. *Rev Neurosci* 1999; **10**: 49–57
37. Dehaene S, Kerszberg M, Changeux JP. A neuronal model of a global workspace in effortful cognitive tasks. *Proc Natl Acad Sci U S A* 1998; **95**: 14529–34
38. Mashour GA, Roelfsema P, Changeux JP, Dehaene S. Conscious processing and the global neuronal workspace hypothesis. *Neuron* 2020; **105**: 776–98
39. Qin P, Di H, Liu Y, et al. Anterior cingulate activity and the self in disorders of consciousness. *Hum Brain Mapp* 2010; **31**: 1993–2002
40. Huang Z, Zhang J, Wu J, Mashour GA, Hudetz AG. Temporal circuit of macroscale dynamic brain activity supports human consciousness. *Sci Adv* 2020; **6**: 87–98

Handling editor: Hugh C Hemmings Jr